MAJOR ARTICLE

Phenotypic and Functional Characterization of Human γδ T-Cell Subsets in Response to Influenza A Viruses

Gang Qin,[1,3,a] Yinping Liu,[1,a] Jian Zheng,[1] Zheng Xiang,[1] Iris H. Y. Ng,[1,2] J. S. Malik Peiris,[2] Yu-Lung Lau,[1] and Wenwei Tu[1]

[1]Departments of Paediatrics and Adolescent Medicine, and [2]Department of Microbiology, Li Ka Shing Faculty of Medicine, University of Hong Kong, Hong Kong SAR; and [3]Department of Infectious Diseases, Nantong Third People's Hospital, Nantong University, China

Like αβ T cells, human γδ T cells also have different subsets with distinct characteristics. Whether human Vγ9Vδ2 T cells have functionally different subsets in response to influenza A (fluA) viruses remains unknown. In this study, we show for the first time that both central ($CD45RA^-CD27^+$) and effector ($CD45RA^-CD27^-$) memory Vγ9Vδ2 T cells have similar levels of immediate interferon (IFN) γ and cytotoxic responses to human and avian fluA virus–infected cells. In contrast, $CD56^+$ Vγ9Vδ2 T cells have significantly higher cytotoxicity against fluA virus–infected cells compared with their $CD56^-$ counterparts, whereas both subsets have similar IFN-γ responses. We further demonstrate that the CD16-dependent degranulation pathway, but not antibody-dependent cell-mediated cytotoxicity, contribute to the superior cytotoxicity of $CD56^+$ Vγ9Vδ2 T cells. Our study provides further evidence for the phenotypic and functional characterization of human Vγ9Vδ2 T-cell subsets during fluA virus infection and may help improve the γδ T-cell–based immunotherapy for viral infection.

It has become increasingly clear that γδ T cells are important components in both innate and adaptive immune systems, yet the cellular requirement for the activation of γδ T cells is still poorly defined. Like αβ T cells, human Vγ9Vδ2 T cells can be divided into 4 subsets: naive, central memory, effector memory, and terminal differentiated cells, according to their surface expression of CD45RA and CD27 [1–4]. Naive ($CD45RA^+CD27^+$) and central memory ($CD45RA^-CD27^+$) Vγ9Vδ2 T cells tend to locate in the lymph nodes and lack immediate effector functions. Effector memory ($CD45RA^-CD27^-$) and terminally differentiated ($CD45RA^+CD27^-$) Vγ9Vδ2 T cells prefer to locate at the inflammatory sites and can exhibit immediate effector functions [5]. Distinct memory phenotypes of γδ T cells may exhibit differential functions [5–7] and be associated with some diseases such as pulmonary tuberculosis [8]. For influenza A (fluA) virus infection, the differentiation of γδ T cells and their functions remain unclear.

CD56, a calcium-independent neural cell adhesion molecule [9], is a signature marker for natural killer (NK) cells and has also been identified on other cells such as cytotoxic αβ T cells and γδ T cells [10]. The expression of CD56 on cytotoxic lymphocytes is usually associated with lack of major histocompatibility complex (MHC) restriction and reduced T cell receptor dependence [11]. However, little is known about the functions of $CD56^+$ and $CD56^-$ γδ T-cell subsets in fluA virus infection.

In our previous studies, we demonstrated that human Vγ9Vδ2 T cells are potent killers of fluA virus–infected cells and that γδ T-cell–based immunotherapy is an alternative for treating fluA infection [12–14]. In this study, we further evaluate different subsets of

Received 19 August 2011; accepted 5 December 2011; electronically published 28 March 2012.

[a]G. Q. and Y. L. contributed equally to this study.

Correspondence: Wenwei Tu, MD & PhD, Department of Paediatrics and Adolescent Medicine, Li Ka Shing Faculty of Medicine, University of Hong Kong, Room L7-56, 7/F Laboratory Block, Faculty of Medicine Bldg, 21 Sassoon Rd, Hong Kong SAR, China (wwtu@hkucc.hku.hk).

The Journal of Infectious Diseases 2012;205:1646–53

DOI: 10.1093/infdis/jis253

isopentenyl pyrophosphate (IPP)–expanded Vγ9Vδ2 T cells according to their memory types (CD27 expression or CD56 expression) and compare their functions in response to fluA viruses.

MATERIALS AND METHODS

Cells

Peripheral blood mononuclear cells (PBMCs) were isolated from buffy coats of healthy donors (from Hong Kong Red Cross) by Ficoll-Hypaque (Pharmacia) gradient centrifugation. The research protocol was approved by the Institutional Review Board of the University of Hong Kong. The IPP-expanded Vγ9Vδ2 T cells were generated as described elsewhere [12]. Briefly, PBMCs were cultured in Roswell Park Memorial Institute 1640 medium supplemented with 10% fetal bovine serum. IPP (Sigma) was added at days 0 and 3 to a final concentration of 6 μg/mL. Recombinant human interleukin 2 (IL-2) (Invitrogen) was added to a final concentration of 500 IU/mL every 3 days starting on day 3. After 14 days of culture, the cells were purified by negative selection with a TCR γ/δ^+ T-cell isolation kit according to manufacturer's instructions (Miltenyi Biotec). The purity of γδ T cells, as determined by flow cytometry with anti-CD3 and anti-Vδ2 monoclonal antibodies (mAbs), was consistently >98%.

Human monocyte-derived macrophages (MDMs) were generated from PBMCs, as described elsewhere [15]. Briefly, the monocytes were seeded into the 24-well plates and cultured for 14 days to differentiate into macrophages. The purity of monocytes, as determined by flow cytometry with anti-CD14 mAb, was consistently >90%.

fluA Viruses

As described in a previous study [15], human seasonal fluA virus H1N1 (A/Hong Kong/54/98) and avian H9N2 (A/Quail/HK/G1/97), avian H5N1 (A/HK/483/97) were cultured in Madin-Darby canine kidney cells (American Type Culture Collection). Pandemic H1N1 (A/California/04/2009, pdmH1N1) was propagated in embryonated chicken eggs. The viruses were concentrated and purified over a sucrose step gradient, as described elsewhere [16]. The virus titer was determined by daily observation of cytopathic effect, and 50% median tissue culture infective dose was calculated according to the Reed-Muench formula. MDMs were infected with the above fluA virus at a multiplicity of infection of 2. After 1 hour, the unadsorbed virus was washed away.

Flow Cytometry

Cells were stained for surface markers with the following mAbs: anti-Vδ2 (B6), anti-CD3 (HIT3a), anti-CD16 (3G8), anti-CD27 (O323), anti-CD56 (HCD56), anti-CD69 (FN50), and anti-FasL (NOK-1) (Biolegend), and anti-CD27 (M-T271), anti-CD45RA (HI100), anti-CD62L (DREG-56), anti-CD107a (H4A3), and anti-NKG2D (1D11) (BD Biosciences). Intracellular staining was performed after cell fixation and permeabilization, as described elsewhere [17–19], and the following mAbs were used: anti–IFN-γ (25723.11; BD Biosciences) and anti-perforin (dG9) and anti–granzyme B (GB11) antibodies (Biolegend). All samples were acquired on BD FACSAria (BD Biosciences) and analyzed using Flowjo software version 8.8.6 (Tree Star).

After culture for 14 days, different γδ T-cell subsets were sorted with FACSAria-II (BD) dependent on the surface expression levels of CD27 or CD56. The isolated γδ T-cell subsets were routinely >97% pure by flow cytometric analysis.

Cytotoxicity Assay and Relevant Blocking Assay

The cytotoxicity assay of expanded γδ cells was performed with allophycocyanin-conjugated anti-CD3 mAb and EthD-2, as described elsewhere [12, 13]. In brief, MDMs (target) infected with fluA virus were cocultured with autologous IPP-expanded Vγ9Vδ2 T cells (effector) at different effector-to-target (E/T) ratios for 4–6 hours. Afterward, nonadherent cells were harvested directly. Adherent cells were detached with 0.25% (wt/vol) trypsin–0.53 mmol/L ethylenediaminetetraacetic acid. All cells were then stained with anti-CD3 to identify γδ T cells and EthD-2 to identify dead cells [20]. The cytotoxicity of γδ T cells against virus-infected MDMs was assessed by flow cytometry as the percentage of EthD-2^+ cells in the $CD3^-$ population.

For cytotoxicity blocking assays, γδ T cells (effector) were pretreated with anti-CD16 (10 μg/mL; 3G8, Biolegend) neutralization antibody or its isotype control mouse immunoglobulin G1 (IgG1) (10 μg/mL; Biolegend) for 30 minutes. These γδ T cells were then cocultured with virus-infected MDMs (target) at an E/T ratio of 10:1 for 6 hours. Cytotoxicity was analyzed by flow cytometry, as described above.

Statistical Analysis

Data were expressed as means ± standard errors of the mean. Statistical significance was determined by paired Student *t* test, using GraphPad Prism version 5 software. Differences were considered significant at $P < .05$.

RESULTS

Comparable IFN-γ Response and Cytotoxic Activity Between $CD27^+$ and $CD27^-$ γδ T-Cell Subsets to fluA Viruses

We first examined whether peripheral resting Vγ9Vδ2 T cells differentiated toward different memory phenotypes after IPP expansion. As shown in Figure 1*A*, about 80% of peripheral resting γδ T cells showed memory phenotypes, evidenced by the loss of CD45RA. In contrast, the majority (>95%) of IPP-expanded Vγ9Vδ2 T cells were $CD45RA^-$, composed of central ($CD27^+$) and effector memory ($CD27^-$) phenotypes. In addition, these IPP-expanded Vγ9Vδ2 T cells, either $CD27^+$ or

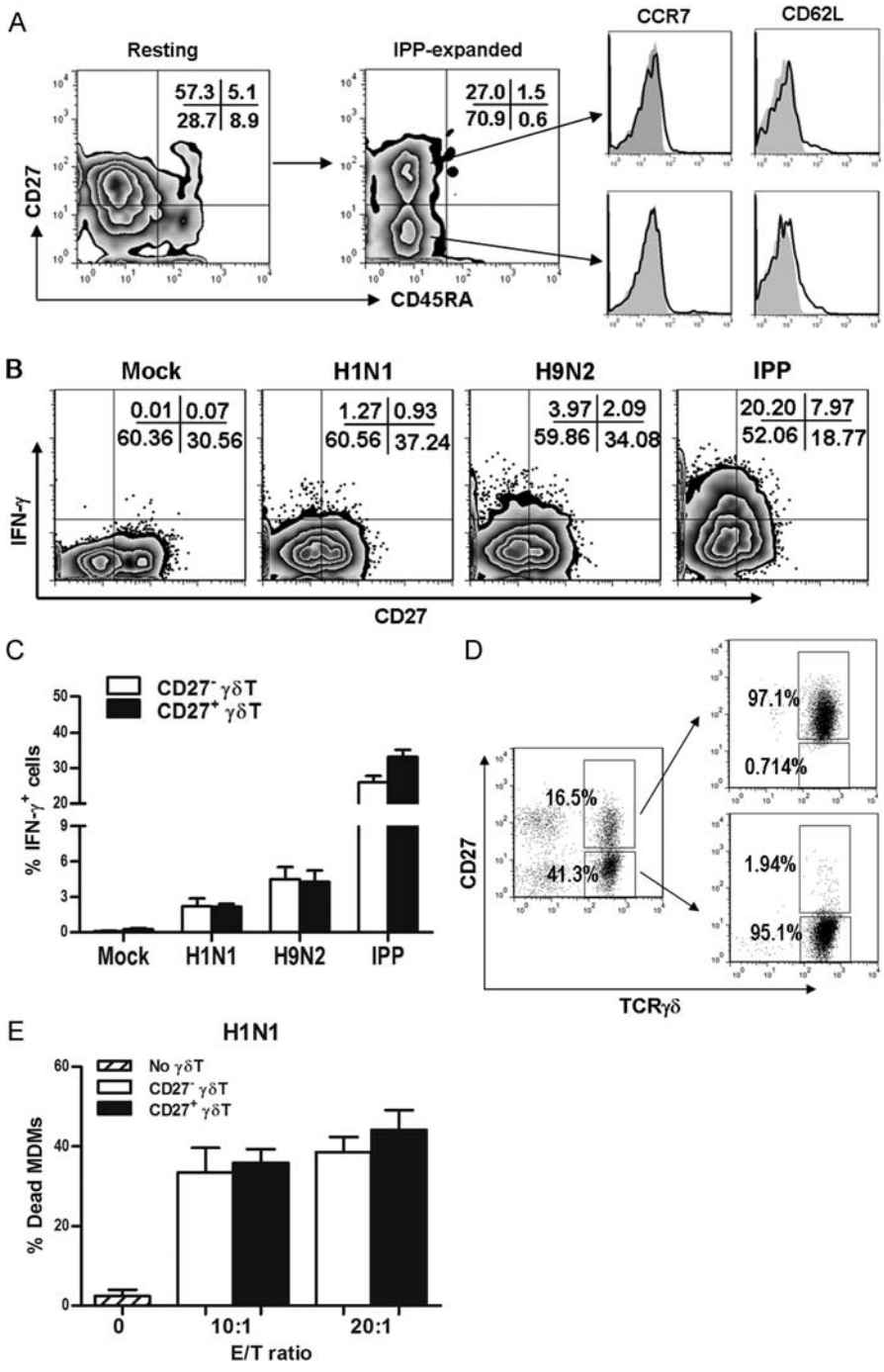

Figure 1. Interferon (IFN) γ response and cytotoxic activity between $CD27^+$ and $CD27^-$ γδ T-cell subsets to influenza A viruses. *A,* Phenotypes of Vγ9Vδ2 T cells in freshly isolated peripheral blood mononuclear cells (PBMCs) and isopentenyl pyrophosphate (IPP)–expanded cells. Results shown were representative of 4 experiments. Gray histograms depict isotype controls. *B,C,* Vγ9Vδ2 T cells were expanded with IPP for 14 days and then cocultured with mock H1N1 or H9N2 virus–infected autologous monocyte-derived macrophages (MDMs) (5×10^5 cells), respectively, at a ratio of 1:1 for 12 hours. IPP-expanded Vγ9Vδ2 T cells cultured with IPP (6 μg/mL) alone were the positive controls. *B,* Intracellular IFN-γ was determined by flow cytometry. *C,* Percentages of IFN-γ^+ cells in $CD27^+$ and $CD27^-$ γδ T-cell subsets are shown in means ± standard errors of the mean (SEMs) (n = 4). *D,* Sorting strategy for isolation of $CD27^+$ and $CD27^-$ Vγ9Vδ2 T-cell subsets from IPP-expanded PBMCs. Abbreviation: TCR, T cell receptor. The purity of sorted cells was consistently above 97%. *E,* Human H1N1 virus–infected MDMs (target) were cocultured with purified autologous $CD27^+$ and $CD27^-$ γδ T cells (effector) at indicated effector-to-target (E/T) ratios for 6 hours. Cytotoxicity was analyzed by flow cytometry and calculated as % dead MDMs. Data shown are means ± SEMs from 4 experiments.

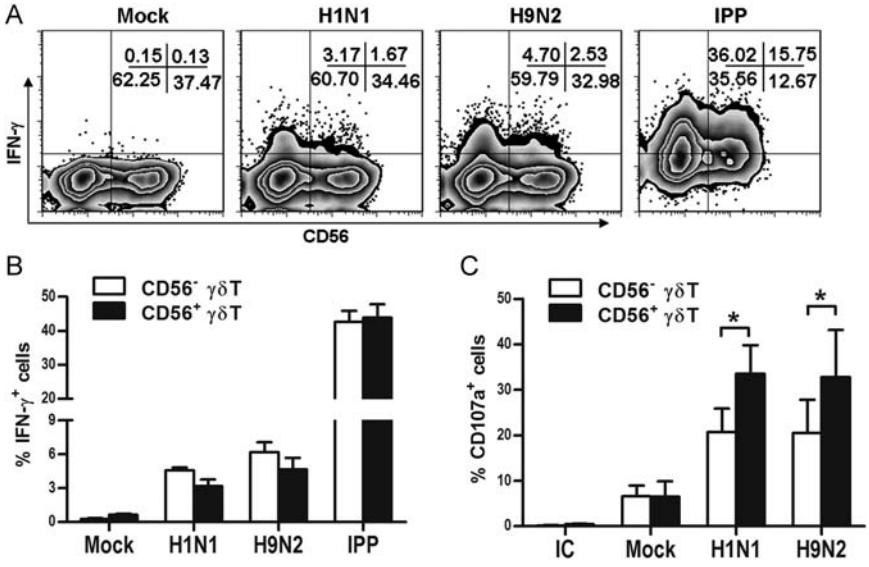

Figure 2. Interferon (IFN) γ production and exocytosis of CD56$^+$ and CD56$^-$ γδ T-cell subsets in response to influenza A viruses. *A, B,* Vγ9Vδ2 T cells were expanded with isopentenyl pyrophosphate (IPP) for 14 days and then cocultured with mock, H1N1 or H9N2 virus–infected autologous monocyte-derived macrophages (MDMs) (5×10^5 cells), respectively, at a ratio of 1:1 for 12 hours. IPP-expanded Vγ9Vδ2 T cells cultured with IPP (6 μg/mL) alone were the positive controls. Intracellular IFN-γ was determined by flow cytometry. *A,* Zebra plots are representative of 4 experiments. *B,* Percentages of IFN-γ$^+$ cells in CD56$^+$ and CD56$^-$ γδ T-cell subsets were shown as means ± standard errors of the mean (SEMs) ($n = 4$). *C,* IPP-expanded Vγ9Vδ2 T cells were cocultured with mock, H1N1, or H9N2 virus–infected MDMs at a ratio of 10:1 for 4 hours in the presence of fluorescein isothiocyanate–conjugated anti-CD107a monoclonal antibodies. Cells were then stained with anti-Vδ2 and anti-CD56 mAbs. IC, isotype control antibody. Data are expressed as means ± SEMs from 4 experiments. The 2-tailed paired Student *t* test was used for comparisons; *$P < .05$.

CD27$^-$, expressed few lymph node homing markers, CCR7 and CD62L (Figure 1*A*). These results indicate that on IPP/IL-2 expansion, human peripheral Vγ9Vδ2 T cells tend to differentiate into memory phenotypes.

We then examined the IFN-γ response in CD27$^+$ and CD27$^-$ γδ T-cell subsets on fluA virus infection. As shown in Figure 1*B* and 1*C*, the percentage of IFN-γ$^+$ cells was comparable between CD27$^+$ and CD27$^-$ Vγ9Vδ2 T cells in responses to seasonal human H1N1 virus, avian H9N2 virus, or IPP stimulation. Consistent with our previous findings [13], IPP induced much higher IFN-γ production than fluA viruses. These data indicate that central (CD45RA$^-$CD27$^+$) and effector memory (CD45RA$^-$CD27$^-$) Vγ9Vδ2 T cells have similar capacity to produce IFN-γ in response to fluA viruses or phosphoantigen.

To further compare the cytotoxic capacity of CD27$^+$ and CD27$^-$ Vγ9Vδ2 T-cell subsets, we sorted these 2 populations by using FACSAria flow cytometry (Figure 1*D*) and determined their cytotoxic activity. As shown in Figure 1*E*, both CD27$^+$ and CD27$^-$ γδ T-cell subsets killed human seasonal H1N1 virus–infected MDMs efficiently. However, there was no significant difference between the cytotoxic activities of CD27$^+$ and CD27$^-$ Vγ9Vδ2 T-cell subsets, whether the E/T ratio was 10:1 or 20:1. The results indicate that the anti-fluA cytotoxic functions of central and effector memory Vγ9Vδ2 T cells are similar.

IFN-γ Response and Exocytosis of CD56$^+$ and CD56$^-$ γδ T-Cell Subsets to fluA Virus Infection

Human Vγ9Vδ2 T cells can be divided into 2 subsets: CD56$^+$ and CD56$^-$ cells (Figure 3*A*). Because CD56 expression on stimulated αβ T cells is thought to be associated with differentiated effector functions [21–23], we examined CD56$^+$ and CD56$^-$ Vγ9Vδ2 T-cell subsets to determine whether they have differential IFN-γ responses to fluA virus infections. As shown in Figure 2*A* and 2*B*, on seasonal H1N1 virus stimulation, the percentage of IFN-γ$^+$ cells was comparable between CD56$^+$ and CD56$^-$ Vγ9Vδ2 T cells. Similar results were observed between these 2 subsets in response to avian fluA H9N2 virus and phosphoantigen IPP. Consistent with our previous findings [13], IPP induced much higher IFN-γ production than fluA viruses. These results suggest that the CD56$^+$ and CD56$^-$ Vγ9Vδ2 T-cell subsets have similar IFN-γ responses with fluA virus or phosphoantigen stimulation.

The expression of CD107a (lysosome-associated membrane protein 1), a marker for exocytosis of granules, was also assessed. As shown in Figure 2*C*, the coculture of purified Vγ9Vδ2 T cells with H1N1-infected MDMs for 4 hours resulted in a significant increase in CD107a expression in CD56$^+$ Vγ9Vδ2 T cells compared with that in CD56$^-$ cells. Similar results were also observed in these subsets upon H9N2 virus stimulation (Figure 2*C*). These data indicate that the

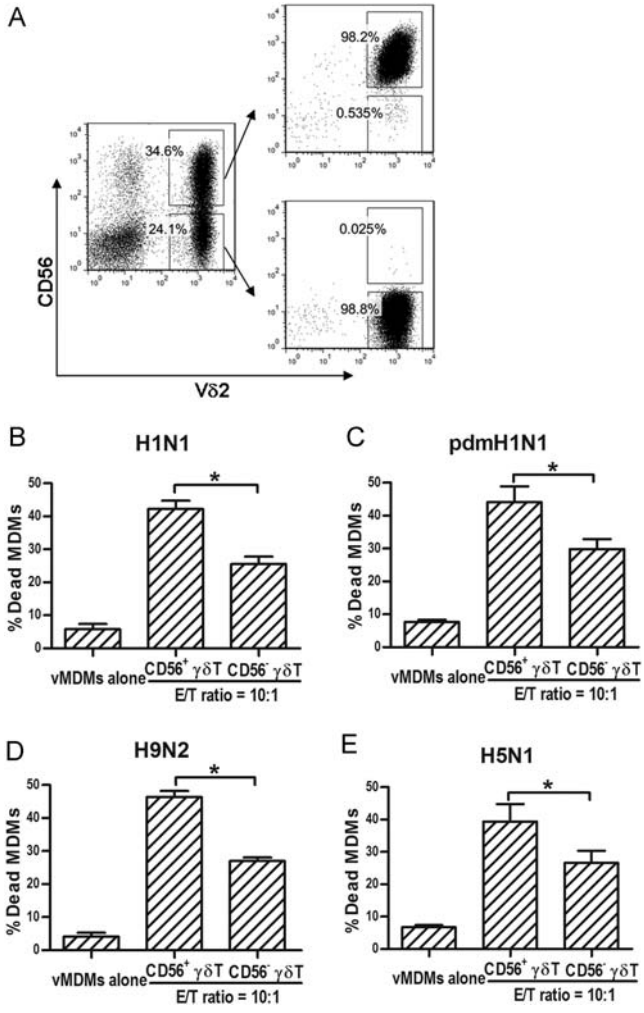

Figure 3. Cytotoxicity of CD56$^+$ and CD56$^-$ γδ T-cell subsets against influenza A virus–infected monocyte-derived macrophages (MDMs). *A,* Sorting strategy of CD56$^+$ and CD56$^-$ Vγ9Vδ2 T-cell subsets from isopentenyl pyrophosphate–expanded peripheral blood mononuclear cells. The purity of sorted cells was consistently above 97%. *B–E,* MDMs (target) infected with human seasonal H1N1 (*B*), pandemic H1N1 (*C*), avian H9N2 (*D*), or H5N1 (*E*) virus were cocultured with purified autologous CD56$^+$ and CD56$^-$ Vγ9Vδ2 T cells (effector) at an effector-to-target (E/T) ratio of 10:1 for 6 hours. Cytotoxicity was analyzed by flow cytometry and calculated as % dead MDMs. Data shown are mean ± standard error of the mean from 4 experiments. The 2-tailed paired Student *t* test was used for comparisons; **P* < .05.

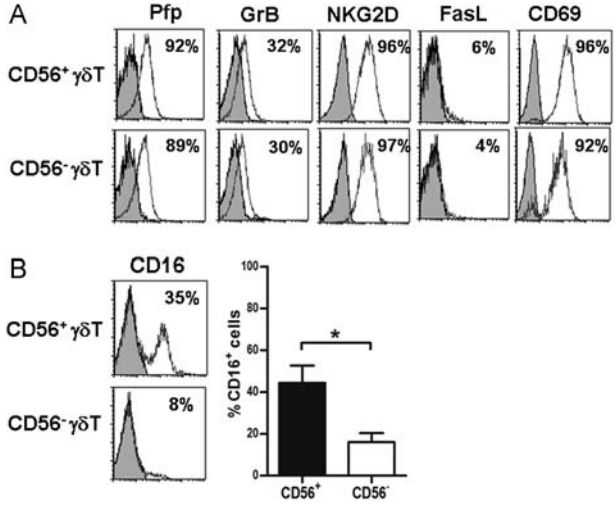

Figure 4. Phenotypic characterization of CD56$^+$ and CD56$^-$ γδ T-cell subsets. *A,* White histograms depict surface expression of NKG2D, Fas ligand (FasL), CD69, intracellular perforin (Pfp), and granzyme B (GrB) of isopentenyl pyrophosphate–expanded CD56$^+$ and CD56$^-$ Vγ9Vδ2 T cells. Gray histograms depict isotype controls. Data are representative of 4 experiments. *B,* Expression levels of CD16 on CD56$^+$ and CD56$^-$ Vγ9Vδ2 T-cell subsets were shown in representative histogram plots and statistic figure with means ± standard errors of the mean (n = 4). Gray histograms depict relevant isotype controls. The 2-tailed paired Student *t* test was used for comparisons; **P* < .05.

exocytosis of the CD56$^+$ Vγ9Vδ2 T-cell subset is stronger than CD56$^-$ counterparts in response to fluA viruses.

Higher Cytotoxicity of CD56$^+$ γδ T Cells Against fluA Virus–Infected MDMs Compared With CD56$^-$ γδ T Cells

To further compare the killing of fluA virus–infected MDMs by CD56$^+$ and CD56$^-$ γδ T cells, highly purified CD56$^+$ and CD56$^-$ Vγ9Vδ2 T-cell subsets were isolated by FACSAria flow cytometry (Figure 3*A*) and their cytotoxic activities were examined. Both CD56$^+$ and CD56$^-$ Vγ9Vδ2 T cells were able to kill fluA virus–infected cells, whether or not human seasonal H1N1, pandemic H1N1, avian H9N2 virus, or avian H5N1 virus were applied (Figure 3*B–E*). However, the cytotoxic ability of CD56$^+$ Vγ9Vδ2 T cells against seasonal H1N1-infected MDMs was significantly higher than that of CD56$^-$ counterparts. Similar differences in the cytotoxic abilities of these 2 subsets against pdmH1N1, H9N2, or H5N1 virus–infected cells were also found (Figure 3*C–E*). These results indicate that CD56$^+$ Vγ9Vδ2 T-cell subsets have superior cytotoxic ability against fluA virus–infected target cells compared with their CD56$^-$ counterparts.

Phenotypes of CD56$^+$ and CD56$^-$ γδ T-Cell Subsets

Our previous study showed that the cytotoxicity of human Vγ9Vδ2 T cells is dependent on the NKG2D activation and is mediated by Fas/Fas ligand (FasL) and perforin-granzyme B pathways [12]. Consequently, we further compared the levels of surface NKG2D and FasL expressions with the intracellular expression of cytotoxic granules for the CD56$^+$ and CD56$^-$ Vγ9Vδ2 T-cell subsets. As shown in Figure 4*A*, CD56$^+$ and CD56$^-$ γδ T-cell subsets expressed similar levels of NKG2D, perforin, granzyme B, and FasL, as well as CD69, which is a recent activation marker. Interestingly, CD56$^+$ Vγ9Vδ2 T cells expressed a significantly higher level of CD16 than did the

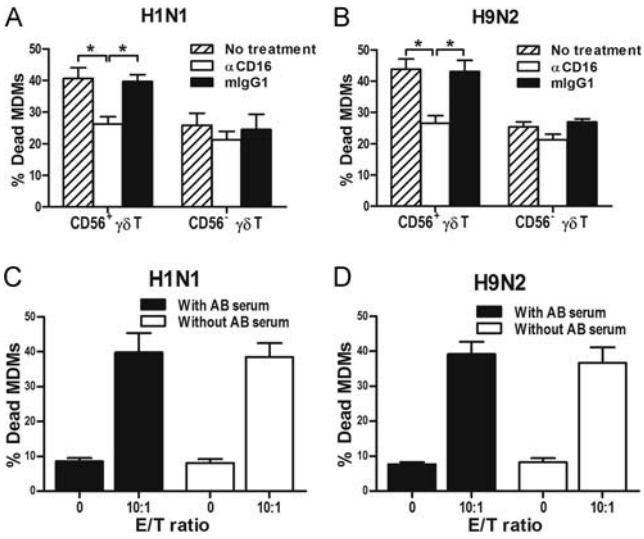

Figure 5. CD16 contributes to the superior cytotoxicity of CD56$^+$ γδ T cells against influenza A virus–infected monocyte-derived macrophages (MDMs). *A, B,* Purified CD56$^+$ and CD56$^-$ Vγ9Vδ2 T cells (effector) were pretreated with anti-CD16 (αCD16, 10 μg/mL) blocking antibody or its isotype control mouse immunoglobulin G1 (mIgG1) (10 μg/mL) for 30 minutes. These Vγ9Vδ2 T cells were then cocultured with H1N1 (*A*) or H9N2 (*B*) virus–infected MDMs (target) at an effector-to-target (E/T) ratio of 10:1 for 6 hours. *C, D,* Purified CD56$^+$ γδ T cells (effector) were cocultured with H1N1 (*C*) or H9N2 (*D*) virus–infected MDMs (target) at an E/T ratio of 10:1 for 6 hours, with or without human AB serum in medium. Cytotoxicity was analyzed by flow cytometry and calculated as % dead MDMs. Data shown are means ± standard errors of the mean from 4 experiments. The 2-tailed paired Student *t* tests was used for comparisons; **P* < .05.

CD56$^-$ counterparts (Figure 4*B*). Because CD16 is thought to be involved in the degranulation of NK cells [24, 25], these data suggest that this higher expression of CD16 in the CD56$^+$ Vγ9Vδ2 T-cell subset may contribute to their superior cytotoxicity against fluA virus–infected cells.

Contribution of CD16 to Superior Cytotoxicity of CD56$^+$ γδ T Cells Against fluA Virus–Infected MDMs

To determine whether the cytotoxic difference between CD56$^+$ and CD56$^-$ Vγ9Vδ2 T-cell subsets was due to the difference in CD16 expression in these cells, CD56$^+$ Vγ9Vδ2 T cells pretreated with the CD16 neutralization mAb were cultured with fluA virus–infected MDMs. For H1N1-infected MDMs, the blockade of CD16 significantly decreased the killing activity of CD56$^+$ Vγ9Vδ2 T cells to the level of their CD56$^-$ counterparts (Figure 5*A*). In contrast, the blockade of CD16 had no such blocking effect on the cytotoxicity of CD56$^-$ cells against H1N1-infected MDMs. Similar results were also observed during the killing of H9N2-infected MDMs by these cells (Figure 5*B*). CD16 is usually associated in antibody-dependent cell-mediated cytotoxicity (ADCC) [26]; therefore, we further sought to examine whether ADCC was involved in the cytotoxicity of CD56$^+$ Vγ9Vδ2 T cells. As shown in Figure 5*C* and 5*D*, CD56$^+$ Vγ9Vδ2 T cells exerted similar cytotoxicity against fluA virus–infected targets, whether they were IgG antibody coated (with AB serum) or not (without AB serum). These results suggest that the supposed serum IgG-mediated ADCC has a negligible effect on the cytotoxicity of CD56$^+$ Vγ9Vδ2 T cells here. Collectively, these results suggest that the CD16-dependent pathway, not ADCC, is responsible for the superior cytotoxicity of CD56$^+$ Vγ9Vδ2 T cells against fluA virus–infected MDMs.

DISCUSSION

Previously we demonstrated that phosphoantigen-expanded human γδ T cells have potent cytotoxicity against fluA virus–infected cells and exhibit type 1 cytokine responses to fluA viruses in vitro [12, 13]. More recently, we found that both the adoptive transfer of phosphoantigen-expanded Vγ9Vδ2 T cells and the use of phosphoantigen to expand Vγ9Vδ2 T cells in vivo can control fluA pathogenesis in a humanized mouse model [14], suggesting γδ T cell-based immunotherapy has a great potential for treating fluA infection. In the current study, we demonstrated for the first time that CD56$^+$ Vγ9Vδ2 T cells are the more potent anti-influenza cytolytic subset compared with their CD56$^-$ counterparts, although their IFN-γ productions are at similar levels. We also showed that central memory (CD45RA$^-$CD27$^+$) γδ T cells display similar immediate response to fluA viruses as effector memory (CD45RA$^-$CD27$^-$) cells in terms of cytotoxicity and IFN-γ production. Therefore, targeting CD56$^+$ rather than whole Vγ9Vδ2 T cells may improve the efficacy of γδ T-cell–based immunotherapy for influenza virus infection.

It is believed that central memory αβ T cells have a greater ability of expansion, whereas effector memory αβ T cells display faster and more potent effector functions [27]. Recent studies suggest that γδ T cells also have central and effector memory subsets. In the mouse model, it has been found that CD27$^+$ γδ TCR thymocytes had much stronger IFN-γ response to PMA and ionomycin stimulation than their CD27$^-$ counterparts [7]. On the contrary, the circulating central memory (CD45RA$^-$CD27$^+$) fraction from an adult healthy donor had less-potent IFN-γ response to IPP than effector memory (CD45RA$^-$CD27$^-$) Vγ9Vδ2 T cells [8]. However, in contrast to the findings described above, we found that IPP-expanded central memory (CD45RA$^-$CD27$^+$) Vγ9Vδ2 T cells were functionally as efficient in cytolytic and IFN-γ responses to fluA viruses as their effector memory (CD45RA$^-$CD27$^-$) counterparts. The difference in effector function between the central and effector memory γδ T cells shown in various studies may be related to the different stage of activation and differentiation of the cells.

Several recent reports suggest that CD56 expression may be associated with differentiated cytolytic effector function not only in conventional αβ T cells but also in γδ T cells [21, 22, 28, 29]. Human intestinal $CD56^+$ T cells have demonstrated stronger IFN-γ–producing ability compared with their $CD56^-$ counterparts [23]. In this study, we observed that the production of IFN-γ by $CD56^+$ and $CD56^-$ Vγ9Vδ2 T cells in response to H1N1, H9N2, or IPP stimulation was at comparable levels. Most importantly, we found that $CD56^+$ Vγ9Vδ2 cells exhibited significantly higher cytotoxic ability against MDMs infected with human seasonal H1N1, pandemic H1N1, avian H9N2 or H5N1 virus, although both $CD56^+$ and $CD56^-$ cells were capable of killing targets. Indeed, a recent study showed that phosphoantigen-expanded $CD56^+$ Vγ9Vδ2 T cells exhibited stronger cytotoxic activity against several solid tumor cells than their $CD56^-$ counterparts [28].

Although CD56 acts as an adhesion molecule in NK–target cell interaction [30] and cross-linking of CD56 induces cell signaling [31] in some contexts, the direct correlation between this molecule and cell-mediated cytotoxicity has not been established [31]. In our previous study, we found that the cytotoxicity of γδ T cells against fluA virus–infected cells is dependent on NKG2D activation and mediated by Fas/FasL and perforin-granzyme B pathways [12]. However, we did not observe a significant difference in the expression levels of NKG2D, perforin, granzyme B, FasL, and CD69 between $CD56^+$ and $CD56^-$ Vγ9Vδ2 T-cell subsets, suggesting that these activation and cytotoxicity-related pathways may not contribute to the superior killing ability of $CD56^+$ γδ T cells against fluA virus–infected cells.

Interestingly, we found that $CD56^+$ γδ T cells expressed significantly higher levels of CD16 compared with their $CD56^-$ counterparts. Furthermore, we demonstrated that CD16 contributed to the superior killing activity of $CD56^+$ γδ T cells, compared with their $CD56^-$ counterparts, against virus-infected MDMs. Indeed, it is thought that CD16 participates in the cell-mediated cytotoxicity of NK, αβ T cells, and even γδ T cells through 3 main pathways: (1) ADCC [26, 32], (2) the CD16-mediated degranulation pathway [24, 25], and (3) acting as a lysis receptor that mediates the killing of some virus-infected and tumor cells independent of antibody ligation [33]. Recently, it has been reported that phosphoantigens could enhance the ADCC function of γδ T cells against tumor cells [34]. However, we demonstrate here that the cytotoxicity of $CD56^+$ γδ T cells against fluA virus–infected cells was not dependent on serum IgG-mediated ADCC. Combined with the evidence that the superior cytotoxicity of $CD56^+$ Vγ9Vδ2 T cells is also associated with higher expression of CD107a, a degranulation marker, our findings indicate that CD16 may be involved in the degranulation pathway of γδ T cells instead of the ADCC pathway, leading to the difference in cytotoxicity of the 2 subsets.

In summary, we found that IPP-expanded $CD56^+$ Vγ9Vδ2 T cells had higher cytotoxicity against virus-infected cells than their $CD56^-$ counterparts, although these 2 subsets had similar IFN-γ responses to fluA viruses. Moreover, the CD16-dependent degranulation pathway contributed to the superior cytotoxicity of the $CD56^+$ γδ T-cell subset. We also showed that both central ($CD45RA^-CD27^+$) and effector ($CD45RA^-CD27^-$) memory γδ T cells had levels of immediate IFN-γ and cytotoxic response that were similar to those of human and avian fluA virus–infected cells. For the first time, our study provides further evidence of the phenotypic and functional characterization of human γδ T-cell subsets during fluA virus infection. Because γδ T-cell–based immunotherapy shows great potential for treating fluA infection, our findings may help improve its efficacy for the control of viral infection.

Notes

Financial support. This work was supported by the Area of Excellence program on influenza supported by the University Grants Committee of the Hong Kong SAR, China (Project AoE/M-12/06); General Research Fund, Research Grants Council of Hong Kong (grants HKU 777108M, HKU777407, HKU768108, HKU781211); and Research Fund for the Control of Infectious Diseases of the Food and Health Bureau of the Hong Kong SAR (grants 07060482 and HK-09-03-05).

Potential conflicts of interest. All authors: No reported conflicts.

All authors have submitted the ICMJE Form for Disclosure of Potential Conflicts of Interest. Conflicts that the editors consider relevant to the content of the manuscript have been disclosed.

References

1. Hoft DF, Brown RM, Roodman ST. Bacille Calmette-Guerin vaccination enhances human gamma delta T cell responsiveness to mycobacteria suggestive of a memory-like phenotype. J Immunol **1998**; 161:1045–54.
2. Dieli F, Sireci G, Di Sano C, et al. Ligand-specific alphabeta and gammadelta T cell responses in childhood tuberculosis. J Infect Dis **2000**; 181:294–301.
3. Shen Y, Zhou D, Qiu L, et al. Adaptive immune response of Vgamma2Vdelta2+ T cells during mycobacterial infections. Science **2002**; 295:2255–8.
4. Chen ZW, Letvin NL. Adaptive immune response of Vgamma2Vdelta2 T cells: a new paradigm. Trends Immunol **2003**; 24:213–9.
5. Dieli F, Poccia F, Lipp M, et al. Differentiation of effector/memory Vdelta2 T cells and migratory routes in lymph nodes or inflammatory sites. J Exp Med **2003**; 198:391–7.
6. Eberl M, Engel R, Beck E, Jomaa H. Differentiation of human gamma-delta T cells towards distinct memory phenotypes. Cell Immunol **2002**; 218:1–6.
7. Ribot JC, deBarros A, Pang DJ, et al. CD27 is a thymic determinant of the balance between interferon-gamma- and interleukin 17-producing gammadelta T cell subsets. Nat Immunol **2009**; 10:427–36.
8. Gioia C, Agrati C, Casetti R, et al. Lack of CD27-CD45RA-V gamma 9V delta 2+ T cell effectors in immunocompromised hosts and during active pulmonary tuberculosis. J Immunol **2002**; 168:1484–9.
9. Cunningham BA, Hemperly JJ, Murray BA, Prediger EA, Brackenbury REdelman GM. Neural cell adhesion molecule: structure, immunoglobulin-like domains, cell surface modulation, and alternative RNA splicing. Science **1987**; 236:799–806.
10. Satoh M, Seki S, Hashimoto W, et al. Cytotoxic gammadelta or alphabeta T cells with a natural killer cell marker, CD56, induced from

human peripheral blood lymphocytes by a combination of IL-12 and IL-2. J Immunol **1996**; 157:3886–92.
11. Schmidt RE, Murray C, Daley JF, Schlossman SF, Ritz J. A subset of natural killer cells in peripheral blood displays a mature T cell phenotype. J Exp Med **1986**; 164:351–6.
12. Qin G, Mao H, Zheng J, et al. Phosphoantigen-expanded human gammadelta T cells display potent cytotoxicity against monocyte-derived macrophages infected with human and avian influenza viruses. J Infect Dis **2009**; 200:858–65.
13. Qin G, Liu Y, Zheng J, et al. Type 1 responses of human Vgamma9V-delta2 T cells to influenza A viruses. J Virol **2011**; 85:10109–16.
14. Tu W, Zheng J, Liu Y, et al. The aminobisphosphonate pamidronate controls influenza pathogenesis by expanding a γδ T cell population in humanized mice. J Exp Med **2011**; 208:1511–22.
15. Tu W, Mao H, Zheng J, et al. Cytotoxic T lymphocytes established by seasonal human influenza cross-react against 2009 pandemic H1N1 influenza virus. J Virol **2010**; 84:6527–35.
16. Arora DJ, Tremblay P, Bourgault R, Boileau S. Concentration and purification of influenza virus from allantoic fluid. Anal Biochem **1985**; 144:189–92.
17. Mao H, Tu W, Liu Y, et al. Inhibition of human natural killer cell activity by influenza virions and hemagglutinin. J Virol **2010**; 84: 4148–57.
18. Zheng J, Liu Y, Qin G, et al. Efficient induction and expansion of human alloantigen-specific CD8 regulatory T cells from naive precursors by CD40-activated B cells. J Immunol **2009**; 183:3742–50.
19. Zheng J, Liu Y, Qin G, et al. Generation of human Th1-like regulatory CD4(+) T cells by an intrinsic IFN-γ- and T-bet-dependent pathway. Eur J Immunol **2011**; 41:128–39.
20. King MA. Detection of dead cells and measurement of cell killing by flow cytometry. J Immunol Methods **2000**; 243:155–66.
21. Casado JG, Soto R, DelaRosa O, et al. CD8 T cells expressing NK associated receptors are increased in melanoma patients and display an effector phenotype. Cancer Immunol Immunother **2005**; 54:1162–71.
22. Pittet MJ, Speiser DE, Valmori D, Cerottini JC, Romero P. Cutting edge: cytolytic effector function in human circulating CD8+ T cells closely correlates with CD56 surface expression. J Immunol **2000**; 164:1148–52.
23. Cohavy O, Targan SR. CD56 marks an effector T cell subset in the human intestine. J Immunol **2007**; 178:5524–32.
24. Bryceson YT, March ME, Barber DF, Ljunggren HG, Long EO. Cytolytic granule polarization and degranulation controlled by different receptors in resting NK cells. J Exp Med **2005**; 202:1001–12.
25. Das A, Long EO. Lytic granule polarization, rather than degranulation, is the preferred target of inhibitory receptors in NK cells. J Immunol **2010**; 185:4698–704.
26. Trotta R, Puorro KA, Paroli M, et al. Dependence of both spontaneous and antibody-dependent, granule exocytosis-mediated NK cell cytotoxicity on extracellular signal-regulated kinases. J Immunol **1998**; 161:6648–56.
27. Sprent J, Surh CD. T cell memory. Annu Rev Immunol **2002**; 20: 551–79.
28. Alexander AA, Maniar A, Cummings JS, et al. Isopentenyl pyrophosphate-activated CD56+ γδ T lymphocytes display potent antitumor activity toward human squamous cell carcinoma. Clin Cancer Res **2008**; 14:4232–40.
29. Urban EM, Li H, Armstrong C, Focaccetti C, Cairo C, Pauza CD. Control of CD56 expression and tumor cell cytotoxicity in human Vgamma2Vdelta2 T cells. BMC Immunol **2009**; 10:50.
30. Nitta T, Yagita H, Sato K, Okumura K. Involvement of CD56 (NKH-1/Leu-19 antigen) as an adhesion molecule in natural killer-target cell interaction. J Exp Med **1989**; 170:1757–61.
31. Lanier LL, Chang C, Azuma M, Ruitenberg JJ, Hemperly JJ, Phillips JH. Molecular and functional analysis of human natural killer cell-associated neural cell adhesion molecule (N-CAM/CD56). J Immunol **1991**; 146:4421–6.
32. Chen Z, Freedman MS. CD16+ gammadelta T cells mediate antibody dependent cellular cytotoxicity: potential mechanism in the pathogenesis of multiple sclerosis. Clin Immunol **2008**; 128:219–27.
33. Mandelboim O, Malik P, Davis DM, Jo CH, Boyson JE, Strominger JL. Human CD16 as a lysis receptor mediating direct natural killer cell cytotoxicity. Proc Natl Acad Sci USA **1999**; 96:5640–4.
34. Gertner-Dardenne J, Bonnafous C, Bezombes C, et al. Bromohydrin pyrophosphate enhances antibody-dependent cell-mediated cytotoxicity induced by therapeutic antibodies. Blood **2009**; 113:4875–84.